OMICS A Journal of Integrative Biology
Volume 14, Number 6, 2010

DOI: 10.1089/omi.2010.0041

Phospholipidome of *Candida*: Each Species of *Candida* Has Distinctive Phospholipid Molecular Species

Ashutosh Singh,[1] Tulika Prasad,[2] Khyati Kapoor,[1] Ajeet Mandal,[1] Mary Roth,[3] Ruth Welti,[3] and Rajendra Prasad[1]

Abstract

By employing electrospray ionization tandem mass spectrometry (ESI-MS/MS), the phospholipidomes of eight hemiascomycetous human pathogenic *Candida* species have been characterized. Over 200 phospholipid molecular species were identified and quantified. There were no large differences among *Candida* species in phosphoglyceride class composition; however, differences in phosphoglycerides components (i.e., fatty acyl chains) were identified. In contrast, differences in sphingolipid class composition as well as in molecular species were quite evident. The phospholipid compositions of *C. albicans, C. glabrata, C. parapsilosis*, *C. kefyr*, *C. tropicalis, C. dubliniensis, C. krusei,* and *C. utilis* could be further discriminated by principal component analysis. Notwithstanding that a single strain of each species was analyzed, our data do point to a typical molecular species imprint of *Candida* strains.

Introduction

Several antifungal drugs target enzymes involved in lipid biosynthesis in *Candida*. Use of these drugs invariably leads to the development of multidrug resistance (MDR) (Prasad and Kapoor, 2005). Membrane lipid metabolism and physical properties appear to be closely linked to MDR in *Candida* (Mukhopadhyay et al., 2002). For example, changes in membrane lipid phase and asymmetry affect azole resistance (Kohli et al., 2002). Indeed, the drug susceptibility phenotype of *Candida* appears to result from interplay among drug diffusion, drug extrusion, and the membrane lipid environment (Mukhopadhyay et al., 2004; Pasrija et al., 2005, 2008).

Although lipid metabolic pathways are fairly well established in yeast (Gasper et al., 2007), our knowledge of lipid compositional profile, particularly in *Candida* species, is rather limited (Mago and Khuller, 1990a, 1990b; Mahmoudabadi et al., 2001; Van et al., 2008). Employing classical analytical methods, Dembitskii and Pechenkina (1991) analyzed phospholipid (PL) and fatty-acid (FA) compositions of nine species of fungi, identifying and quantifying major classes of lipids. Phosphatidylcholine (PC) and phosphatidylethanolamine (PE) were found to be the main classes of phosphoglycerides, followed by phosphatidylserine (PS), phosphatidylinositol (PI), phosphatidylglycerol (PG), and cardiolipin (CL). The introduction of high-throughput analyses of PLs, recently performed on nonpathogenic *Saccharomyces cerevisiae,* is accelerating our ability to analyze yeast lipid metabolism and signaling, and the factors that regulate them (Ejsing et al., 2009; Guan and Wenk, 2006).

Lipidomics is a branch of metabolomics that provides a systematic approach to decoding lipid-based information in biosystems (Bleijerveld et al., 2006; Roberts et al., 2008; Watson, 2006; Wenk, 2005). In the present study, eight different *Candida* species, *C. albicans, C. glabrata, C. tropicalis, C. parapsilosis, C. dubliniensis, C. krusei, C. utilis*, and *C. kefyr,* were characterized using profiling based on electrospray ionization (ESI) triple quadrupole mass spectrometry (MS/MS). Nine major phosphoglyceride classes, PC, PE, PS, PG, PI, phosphatidic acid (PA), lysophosphatidylglycerol (LysoPG), lysophosphatidylethanolamine (LysoPE), lysophosphatidylcholine (LysoPC), and three major groups of sphingolipids (SL), inositolphosphorylceramide (IPC), mannosylphosphatidylinositol (MIPC), and mannosyldiinositolphosphorylceramide ($M(IP)_2C$), were analyzed. Employing high-throughput lipid profiling and statistical analyses, we have determined molecular lipid species imprints characteristic of specific *Candida* species.

Materials and Methods

Lipid standards

Synthetic lipids with FA compositions that are not found or are of very low abundance in *Candida* were used as internal

[1]Membrane Biology Laboratory, School of Life Sciences, Jawaharlal Nehru University, New Delhi, India.
[2]Advanced Instrumentation Research Facility, Jawaharlal Nehru University, New Delhi, India.
[3]Kansas Lipidomics Research Center, Division of Biology, Ackert Hall, Kansas State University, Manhattan, KS, USA.

standards. Lipid standards were obtained from Avanti Polar Lipids (Alabaster, AL, USA).

Strains, media and culture conditions

Candida strains used in this study are listed in Table 1. *Candida* cells were kept on YPD plates and inoculated in YPD medium (1% yeast extract, 2% glucose, and 2% bactopeptone). The cells were diluted into 50 mL fresh medium at 0.1 OD ($\sim 10^6$ cells/mL) at A_{600} and grown for 14 h until the cells reached exponential growth ($\sim 2\times 10^8$ cells/mL). Three separate cultures of each *Candida* strain were used.

Lipid extraction

Lipids were extracted from *Candida* cells using an earlier described method with slight modification (Bligh and Dyer, 1959). Briefly, the *Candida* cells were harvested at exponential phase and were suspended in 10 mL methanol. Glass beads (4 g) (Glaperlon 0.40–0.60 mm) were added and the suspension was shaken in a cell disintegrator (B. Braun, Melsungen, Germany) four times for 30 s with a gap of 30 s between each shaking. Approximately 20 mL chloroform were added to the suspension to give a ratio of 2:1 of chloroform:methanol (v/v). The suspension was stirred on a flat-bed stirrer at room temperature for 2 h. The suspension was filtered through Whatman No. 1 filter paper, and the extract was transferred to a separatory funnel and washed with 0.2 volumes of 0.9% NaCl to remove the nonlipid contaminants. The aqueous layer was aspirated and the solvent of the lipid-containing, lower organic layer was evaporated under N_2; the lipids were stored at -80°C until analysis.

ESI-MS/MS lipid profiling

Phosphoglyceride quantification. An automated ESI-MS/MS approach was used. Data acquisition and analysis were carried out as described previously with minor modifications (Devaiah et al., 2006). The extracted dry lipid samples were dissolved in 1 mL chloroform (Devaiah et al., 2006). An aliquot of 2 to 8 μL of extract in chloroform was analyzed, with the exact amount depending upon the dry lipid weight of each sample. Previously described precise amounts of internal standards, obtained and quantified (Welti et al., 2002), were added in the following quantities (with some small variation in amounts in different batches of internal standards): 0.6 nmol di12:0-PC, 0.6 nmol di24:1-PC, 0.6 nmol 13:0-LysoPC, 0.6 nmol 19:0-LysoPC, 0.3 nmol di12:0-PE, 0.3 nmol di23:0-PE, 0.3 nmol 14:0-LysoPE, 0.3 nmol 18:0-LysoPE, 0.3 nmol di14:0-PG, 0.3 nmol di20:0(phytanoyl)-PG, 0.3 nmol 14:0-LysoPG, 0.3 nmol 18:0-LysoPG, 0.3 nmol di14:0-PA, 0.3 nmol di20:0(phytanoyl)-PA, 0.2 nmol di14:0-PS, 0.2 nmol di20:0(phytanoyl)-PS, 0.23 nmol 16:0-18:0-PI, and 0.16 nmol di18:0-PI. The sample and internal standard mixture was combined with solvents, such that the ratio of chloroform/methanol/300 mM ammonium acetate in water was 300/665/35 (v/v/v) in a final volume of 1.4 mL. Each phosphoglyceride class was quantified in comparison to the two internal standards of that class.

Unfractionated lipid extracts were directly introduced by continuous infusion into the ESI source on a triple quadrupole MS (API 4000, Applied Biosystems, Foster City, CA, USA). Samples were introduced using an autosampler (LC Mini PAL, CTC Analytics AG, Zwingen, Switzerland) fitted with the required injection loop for the acquisition time and passed to the ESI needle at 30 μL/min.

Sequential precursor (Pre) and neutral loss (NL) scans of the extracts produce a series of spectra revealing a set of lipid species containing a common head group fragment. Lipid species were detected with the following scans: PC and LysoPC, $[M+H]^+$ ions in positive ion mode with Pre 184.1; PE and LysoPE, $[M+H]^+$ ions in positive ion mode with NL 141.0; PA, $[M+NH_4]^+$ in positive ion mode with NL 115.0; PG, $[M+NH_4]^+$ in positive ion mode with NL 189.0; PI, $[M+NH_4]^+$ in positive ion mode with NL 277.0; PS, $[M+H]^+$ in positive ion mode with NL 185.0; LysoPG, $[M-H]^-$ in negative mode with Pre 152.9. The collision gas pressure was set at 2 [arbitrary units (au)]. The collision energies, with nitrogen in the collision cell, were +40 V for PC, +28 V for PE, +25 V for PA, +22 V for PG, PI, and PS, and −57 V for LysoPG. Declustering potentials were +100 V for PC, PE, PA, PG, PI, and PS, and −100 V for LysoPG. Entrance potentials were +14 V for PC, PA, PG, PI, and PS, +15 V for PE, and −10 V for LysoPG. Exit potentials were +14 V for PC, PA, PG, PI, and PS, +11 V for PE, and −14 V for LysoPG. The mass analyzers were adjusted to a resolution of 0.7 U full width at half height. For each spectrum, 9 to 150 continuum scans were averaged in multiple channel analyzer (MCA) mode. The source temperature (heated nebulizer) was 100°C, the interface heater was "on," and +5.5 kV or −4.5 kV were applied to the electrospray capillary. The curtain gas was set at 20 au, and the two ion source gases were set at 45 au.

Processing of the data, including isotope deconvolution, was similar to that described earlier (Devaiah et al., 2006; Welti et al., 2002). The background of each spectrum was subtracted, the data were smoothed, and peak areas integrated using a custom script and Applied Biosystems Analyst

Table 1. *Candida* Strains Used in This Study

Strain	*Genotype*	*Source of reference*
C. albicans CAI4	*Δura3::imm434/Δura3::imm434*	(Fonzi and Irwin, 1993)
C. tropicalis[a] ATCC 750		Ranbaxy Laboratories, India
C. glabrata ATCC 90030		Ranbaxy Laboratories, India
C. parapsilosis ATCC 22019		Ranbaxy Laboratories, India
C. dubliniensis ATCC 33		Ranbaxy Laboratories, India
C. krusei ATCC 6258		Ranbaxy Laboratories, India
C. utilis ATCC 15239		Ranbaxy Laboratories, India
C. kefyr ATCC 2512		Ranbaxy Laboratories, India

[a]ATCC, American Type Culture Collection.

software. The lipids in each class were quantified in comparison to the two internal standards of that class. The first and typically every 11**th** set of mass spectra were acquired on the internal standard mixture only. Peaks corresponding to the target lipids in these spectra were identified and molar amounts calculated in comparison to the internal standards of the same lipid class. To correct for chemical or instrumental noise in the samples, the molar amount of each lipid metabolite detected in the "internal standards only" spectra was subtracted from the molar amount of each metabolite calculated in each set of sample spectra. The data from each "internal standards only" set of spectra were used to correct the data from the following 10 samples. The analyzed data (in nmol) were normalized to the sample's "dry lipid weight" to produce data in the units nmol/mg dry lipid weight. Finally, the data were expressed as mole percent of total lipid analyzed.

Sphingolipid quantification. The ESI-MS/MS procedure for SL quantification was similar to that for phosphoglyceride quantification. Lipid species were detected with the following scans: IPC, $[M-H]^-$ ions in negative ion mode with Pre 259; MIPC, $[M-H]^-$ ions in negative ion mode with Pre 421; $M(IP)_2C$, $[M-H]^-$ in negative mode with Pre 663.1. The internal standard, 16:0–18:1-PI, was detected with $[M+NH_4]^+$ in positive ion mode with NL 277.0, as described in the previous section. The collision gas pressure was set at 2 au. The collision energies, with nitrogen in the collision cell, were -72 V for IPC, -80 V for MIPC, and -75 V for $M(IP)_2C$. The declustering potential was -180 V for IPC, MIPC, and $M(IP)_2C$. The entrance potential was -15 V for IPC, MIPC, and $M(IP)_2C$. The exit potential was -10 V for IPC, MIPC, and $M(IP)_2C$. The mass analyzers were adjusted to a resolution of 0.7 U full width at half height. For each spectrum, 125 to 250 continuum scans were averaged in multiple channel analyzer (MCA) mode. The source temperature (heated nebulizer) was 100°C, the interface heater was "on," and $+5.5$ kV or -4.5 kV were applied to the electrospray capillary. The curtain gas was set at 20 au, and the two ion source gases were set at 45 au. The rest of the processing was similar to that for phosphoglycerides; however, all SL signals were normalized to the signal for 0.23 nmol 16:0–18:0-PI that was added in as an internal standard.

SL amounts were determined by normalizing the mass spectral signal so that a signal of 1.0 represents a signal equal to the signal of 1 nmol 16:0–18:0-PI (the internal standard). These data were then divided by the sample dry lipid weight to obtain signal/dry lipid weight, by the total SL signal to obtain % of total SL signal, or by the total phosphoglyceride + SL signal to obtain % of total phosphoglyceride + SL signal. It is possible that there is variation in ionization efficiency among various SLs and between the internal standard and SL species. Thus, normalized SL species amounts may not reflect their molar amounts. However, the employed procedure allows for determination of relative abundance of SLs and comparison of amounts of particular SLs among samples.

Statistical analysis

The mean of three independent biological replicates ± standard deviation (SD) from the individual samples was used to compare the lipids of *Candida* species. Multivariate data analysis (pattern recognition) was employed. Principal component analysis (PCA) was performed using the software SYSTAT, version 10 (Systat Software Inc., Richmond, CA, USA) using three replicates of each of the eight *Candida* species to highlight the statistically significant lipid differences. To assess the statistical significance of the difference in PC scores, the Student *t*-test was performed using the significance level of 0.05. Hierarchical cluster analysis was also performed using SYSTAT, version 10. When all the values for a particular lipid species were zero in all samples, the data for that lipid species were removed from the analysis. The data in percentage were log-transformed and normalized to the same scale for PCA and hierarchical cluster analysis.

Results

Candida *species have nine major phosphoglycerides*

To evaluate lipid composition, we performed quantitative compositional analysis of each *Candida* species. As described in Materials and Methods, *C. albicans, C. glabrata, C. parapsilosis*, *C. kefyr*, *C. tropicalis, C. dubliniensis, C. krusei*, and *C. utilis* cells were harvested in the exponential growth phase and their total lipids were extracted (Bligh and Dyer, 1959). The extracted lipids were subjected to ESI-MS/MS by direct infusion of the lipid extracts. The total PLs (phosphoglycerides and SLs) were quantified and PL content was found to range between 731 to 932 nmol per mg dry lipid weight in the *Candida* species analyzed (Supplementary Table 1).

MS analysis targeted nine major phosphoglyceride classes in each species of *Candida*; lipid molecular species were identified by mass of the head group plus the mass of the intact lipid, allowing determination of the number of carbon atoms (C atoms) and double bonds in the acyl chain(s) of phosphoglycerides. Phosphoglycerides were quantified in relation to internal standards of the same lipid class. This procedure is known to provide accurate quantification; accurate quantification is possible because various molecular species of the same lipid phosphoglyceride lipid class (here, the internal standard and other species) produce very similar amounts of mass spectral signal after electrospray ionization (Han and Gross, 1994). The order of relative abundance of the diacyl phospholipids, from greatest to least, was PC, PE, PI, PS, PA, and PG, with PC, PE, and PI accounting for ~80% of the phosphoglycerides (Fig. 1 and Supplementary Table 2A). The major phosphoglyceride, PC, ranged from 35% (of the phosphoglycerides) in *C. parapsilosis* to 44% (of the phosphoglycerides) in *C. utilis*. PE ranged from ~22–24% (of the phosphoglycerides) in *C. kefyr*, *C. utilis*, and *C. dubliniensis* to 32% in *C. parapsilosis*. PI content was highest in *C. glabrata* (25% of the phosphoglycerides) and lowest in *C. tropicalis* (13% of the phospholglycerides). The aminophosphoglyceride PS was found to be highest in *C. utilis* and *C. tropicalis* (~9% of the phosphoglycerides) and was only 4% in *C. krusei*. PG contents were very similar among *C. albicans*, *C. tropicalis*, *C. krusei*, *C. kefyr*, and *C. parapsilosis*, ~1% of the phosphoglycerides. PG was ~3% for *C. dubliniensis*, whereas it was <1% in *C. glabrata* and *C. utilis*. PA levels ranged from ~1% to 4% (of the phosphoglycerides) with the highest amount found in *C. dubliniensis* and lowest in *C. krusei*.

Our analysis also targeted three major groups of lysoderivatives of phosphoglycerides that occurred in the order

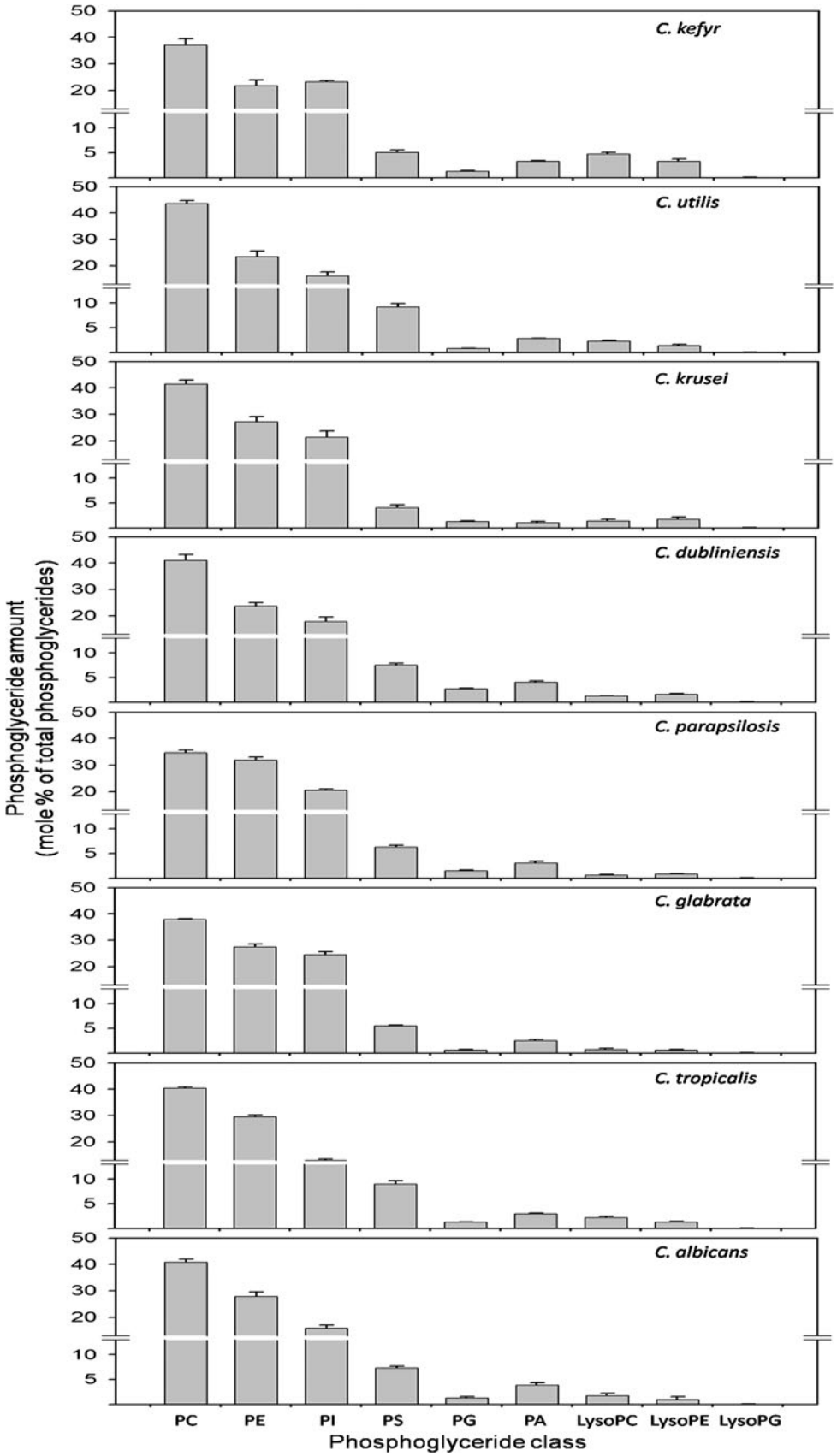

FIG. 1. The mole percentage composition of phosphoglyceride classes in eight *Candida* species. The total for each phosphoglycerides class was calculated by adding the mole percentage of the molecular lipid species of that class. Values are means $\pm$ SD ($n = 3$ for all *Candida* strains).

LysoPC > LysoPE > LysoPG. LysoPC was found to be highest in *C. kefyr* (~5% of the phosphoglycerides) and was lowest in *C. parapsilosis* and *C. glabrata* (~0.7% of the phosphoglycerides). LysoPE was less abundant and varied between ~0.6% and 3% (of the phosphoglycerides). The least abundant lysophosphoglyceride was LysoPG in all *Candida* species (Fig. 1 and Supplementary Table 2).

Analysis of three major sphingolipids

Using MS analysis, we targeted three major groups of SLs, IPC, MIPC, and $M(IP)_2C$, and determined the relative amounts of these lipids. The mass spectral signals of the SLs were normalized to those of a phosphoglyceride internal standard, 16:0–18:0-PI. (use of this internal standard was necessary because standard compounds of each yeast sphingolipid class are not available). The SLs accounted for ~2 to 13% of the total PL mass spectral signal (Fig. 2 and Supplementary Tables 1 and 2B). In *C. tropicalis* and *C. albicans*, total SL levels were several-fold higher than in the other *Candida* species. To evaluate the differences between SLs of *Candida* species, we calculated mole percentage of each class based on total SL normalized mass spectral signal. As is evident from Figure 2B, there were variations in the relative abundance of the SL classes between different *Candida* species. IPCs were detected in all *Candida* species but were particularly high in *C. kefyr* and *C. parapsilosis* (~84 and 96% of total normalized SL mass spectral signal, respectively) and were lowest in *C. glabrata* and *C. albicans* (~31 and 32% of total normalized SL mass spectral signal, respectively). For the rest of *Candida* species IPCs varied between ~48 and 68%. MIPC ranged from ~29 to 69% of total normalized SL mass spectral signal, except in *C. parapsilosis* and *C. kefyr*, where it was between ~2 and 7%, respectively. $M(IP)_2C$ produced less than 4% of the mass spectral signal in most of the species (lowest in *C. glabrata*) except for *C. kefyr* where it was 9%. $M(IP)_2C$ was not detected in *C. krusei*.

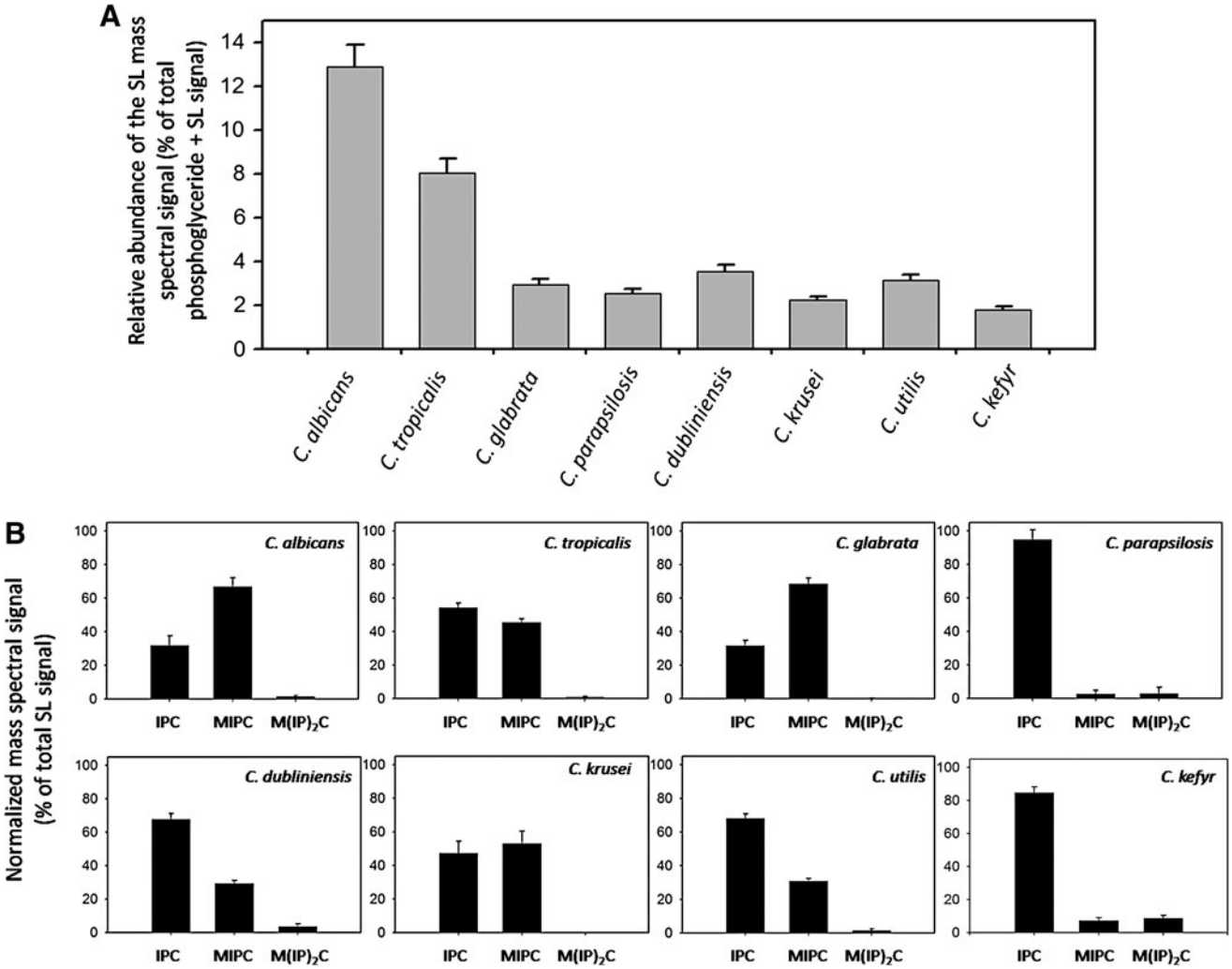

FIG. 2. (**A**) Shows the relative abundance of SLs as mass spectral signal (% of total signal for phosphoglycerides + SL after normalization to internal standards) in eight *Candida* species. (**B**) Shows the relative abundance of SL groups as mole percentage of the normalized total SL mass spectral signal. The total for each SL group was calculated by adding the normalized mass spectral signal of molecular lipid species of that group. Data in tabular form can be found in the Supplementary Table 2. Values are means ± SD ($n = 3$ for all *Candida* strains).

Lipid molecular species

Our analyses thus determined nine phosphoglycerides and three major SLs. These PLs could be further differentiated based on differences in their composition and the degree of unsaturation of their FAs. Lipid profiling by ESI-MS/MS generated data in the form of "number of acyl carbons: number of acyl carbon-carbon double bonds." The numbers of detected phosphoglyceride species for *Candida* were 35, 44, 29, 32, 15, 12, 19, 11, and 6 for PC, PE, PI, PS, PA, LysoPC, PG, LysoPE, and LysoPG, respectively. Notably, PC, which was most abundant on mole percentage basis (Fig. 1), had fewer detectable molecular species (35 species) compared to PE (44 species). To highlight the distribution of molecular species of PL groups, the mole percentage of major molecular species (those with $> 0.01\%$ of total normalized mass spectral signal) are depicted in Figures 3 and 4. The composition of all lipid molecular species is shown in Supplementary Tables 3 and 4.

The PC molecular species included diacyl species with 26 to 40 acyl carbons. These PC species had mono- or di- unsaturation in the lower carbon number PCs, and polyunsaturation was observed for PCs with 34 or more C atoms. Out of 26 major PC species illustrated in Figure 3, PC 34:2, PC 34:3, PC 36:3, and PC 36:4 are the major lipid species in *C. albicans*, *C. tropicalis*, *C. dubliniensis*, *C. krusei,* and *C. kefyr*. Other *Candida* species showed some variations. For example, *C. parapsilosis* had PC 34:3 and PC 36:4 in low abundance, whereas the amounts of less unsaturated PC species such as PC 34:1, PC 36:1, and PC 36:2, were higher. *C. utilis* had lower amounts of PC 34:3 compared to PC 34:1. *C. glabrata*, on the other hand, had only three major PC species: PC 32:2, PC 34:2, and PC 36:2.

The molecular species of PE contained 26 to 44 C atoms with polyunsaturation in the 34, 36, and 40 C atom diacyl species. Among the 27 major PE species, PE 34:1, PE 34:2, PE 34:3, PE 36:2, and PE 36:3 were present in most of the *Candida* species, but in *C. glabrata*, PE 34:2, PE 32:2, and PE 36:2 were the major PE species (Fig. 3). PI (29 species) included molecular species with 26 to 38 C atoms with polyunsaturation observed only in PIs with 34 and 36 acyl carbons. All *Candida* species have PI 34:1 and PI 34:2 as the major PI species. *C. glabrata* and *C. parapsilosis* are rich in PI 36:1 and PI 36:2 species. PS molecular species (32 species) contained 30 to 42 C atoms with PS 34:1 and PS 34:2 being the major PS species in all *Candida* species (Fig. 3). PG molecular species (19 species) contained 30 to 38 C atoms with PG 34:1 and PG 34:2 being the major PG species in all *Candida* species. *C. parapsilosis* and *C. krusei* were rich in PG 36:2 and PG 36:4, respectively. PA molecular species (15 species) contained 32 to 36 C atoms with PA 34:1, PA 34:2, PA36:2, and PA36:3 being the major PA species in all *Candida* species (Fig. 4).

Among the lysophosphoglycerides analyzed (Fig. 5), LysoPC was the most abundant. Twelve species of LysoPC with 14, 15, 16, 17, and 18 acyl C atoms were quantified. LysoPC 16:1, LysoPC 18:1, LysoPC 18:2, and LysoPC 18:3 are the major LysoPCs amongst *Candida* species (Fig. 5). Eleven molecular species of LysoPE were detected with LysoPE 16:0, LysoPE 16:1, LysoPE 18:0, and LysoPE 18:1 as the major lysophosphoglycerides measured in *Candida* species. Six molecular LysoPG species containing 16 and 18 acyl C atoms were analyzed, but these were present in very low amounts.

Using SL profiling by ESI-MS/MS as discussed in Materials and Methods, we determined 21 molecular SL species of IPC (9 species), MIPC (8 species), and $M(IP)_2C$ (4 species) (Fig. 5). SL molecular species are represented as "total number of carbons in the sphingoid base and acyl chains: total number of carbon–carbon double bonds in the sphingoid base and acyl chains; number of hydroxyl groups present in the sphingoid base and acyl chains." Nine IPC species were analyzed for all *Candida* species. IPC species 50:0;3 (*m/z* of $[M - H]^- = 924.6$ U) and 52:0;3 (952.6 U) were the major IPCs except in *C. krusei*, *C. utilis,* and *C. kefyr* where IPC 52:0;4 (968.6 U) was abundant. IPC 52:0;3 (952.6 U) was highest in *C. utilis* and *C. kefyr* ($\sim 55\%$ of total SL signal). Eight MIPC species were detected as $[M - H]^-$ for all *Candida* species. MIPC species 56:0;3 (1086.6 U) and 58:0;3 (1114.7 U) were the major MIPCs in *Candida* except in *C. krusei*, *C. utilis,* and *C. kefyr,* where MIPC 58:0;4 (1130.7 U) was abundant. MIPC 58:0;3 (1114.7 U) was in very high amount in *C. glabrata* (>61% of total SL signal). Four $M(IP)_2C$ molecular species were analyzed for all *Candida* species. $M(IP)_2C$ was not detected in *C. krusei*. $M(IP)_2C$ species 62:0;3 (1329.0 U) and 64:0;3 (1357.0 U) were the major species in *Candida* except in *C. utilis* and *C. glabrata* where $M(IP)_2C$ 62:0;3 (1329 U) was not detected. The importance of these lipidomic differences in differentiating among the *Candida* species was further confirmed by principal component analysis.

Principal component analysis (PCA) of lipid species quantitative data distinctly separates different Candida *species*

PCA is a mathematical algorithm that reduces the dimensionality of the data while retaining most of the variation in the data set (Ringner, 2008). The data are represented by principal components, with the first principal component accounting for the maximum possible variation in the data, and each succeeding component accounting for a portion of the remaining possible variation. Plots allow visual assessment of the similarities and differences among samples and help to determine whether and how samples can be grouped (Devaiah et al., 2006; Ferreira et al., 2010). We performed PCA using the molecular species percentage composition of phosphoglyceride + SL molecular species (data in Supplementary Table 4) to identify and highlight the *Candida* species–specific, statistically significant lipid differences. Analysis allowed the extraction of 21 principal components. The scores of the first three principal components, explaining 52.8% of the total variance, were plotted. Principal components 1, 2, and 3 explained 22.2, 16.9, and 13.7% of the total variance, respectively.

As shown in the plot of principal component 1 versus 2 (Fig. 6A), principal component 1 describes the separation of *C. glabrata* from the other species, particularly from *C. krusei*, *C. dubliniensis,* and *C. tropicalis*. The highest and lowest loading values reflect the lipid species that are most important in the assignment of each principal component (Table 2). Examination of the loadings associated with principal component 1 (Table 2) shows that the content of 30, 32, and 34 carbon phosphoglycerides with two double bonds (PCs 30:2, 32:2, and 34:2, PEs 30:2, 32:2, and 34:2, PA 32:2, and PI 32:2) is important for the separation of *Candida* species along the principal component 1 axis. In fact, each of the molecular

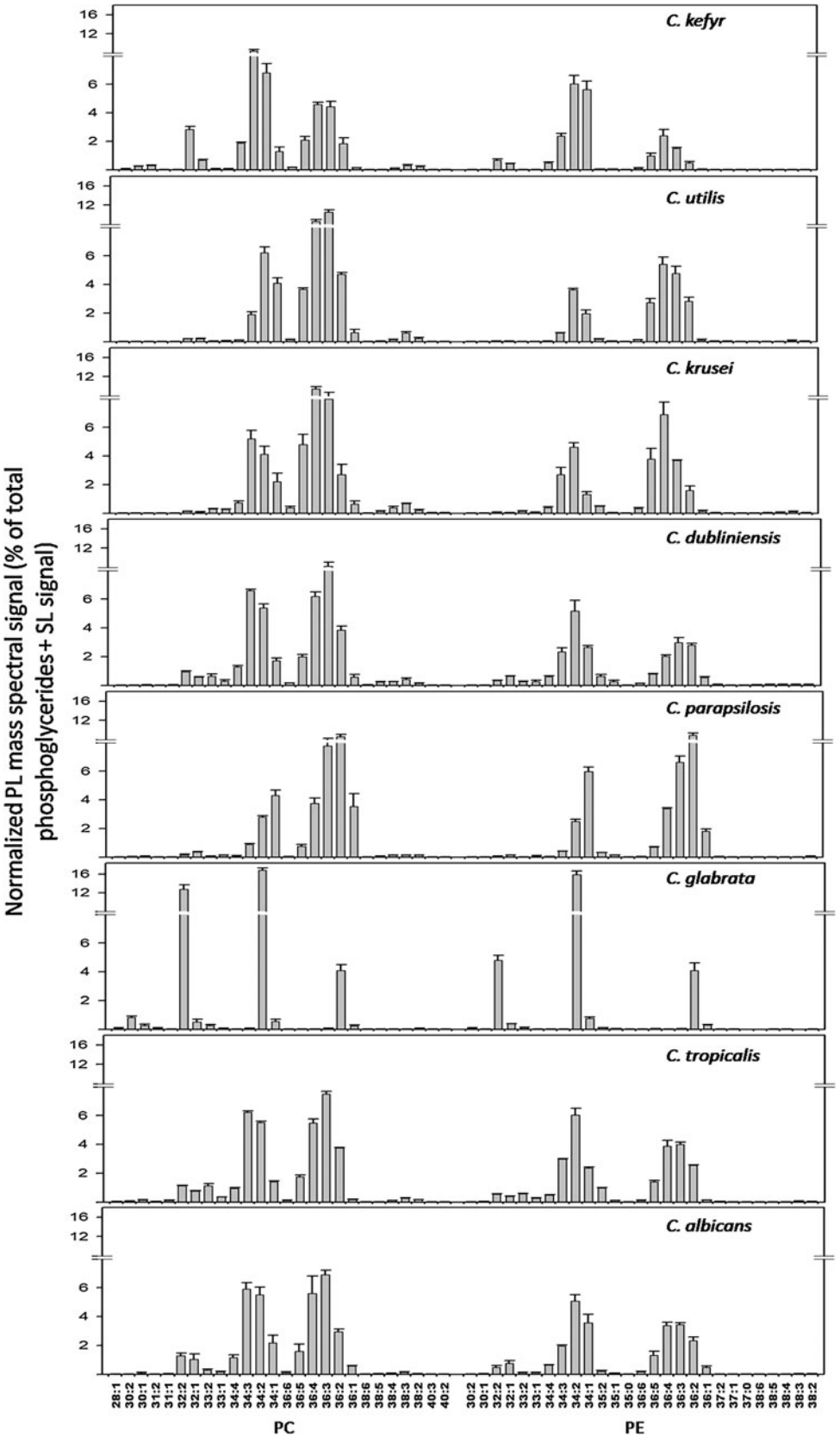

FIG. 3. Molecular lipid species compositions of phosphoglycerides PC and PE (as percentage of the normalized phosphoglyceride + SL mass spectral signals normalized to internal standards) in *Candida*. *Candida* species were cultured in YPD medium at 30°C as described in Materials and Methods. Only the major molecular lipid species (>0.01 mole percentage) are depicted in this figure. Error bars indicate ± SD. ($n = 3$, three independent analyses of lipid extracts from three independent cultures.)

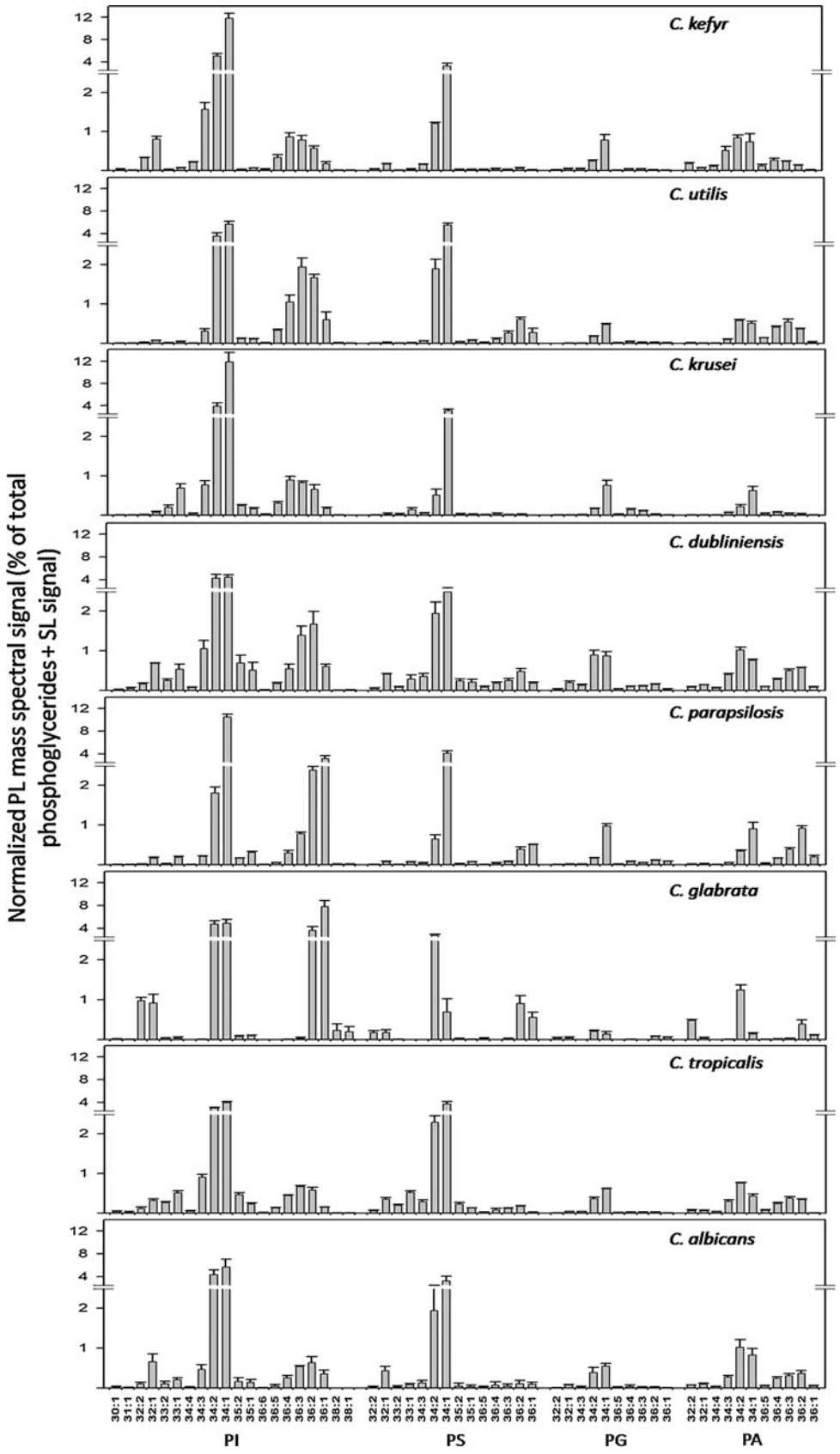

FIG. 4. Molecular lipid species compositions of phosphoglycerides PI, PS, PG, and PA (as percentage of the normalized total phosphoglyceride + SL mass spectral signals normalized to internal standards) in *Candida*. *Candida* species were cultured in YPD medium at 30°C as described in Materials and Methods. Only the major molecular lipid species (>0.01 mole percentage) are depicted in this figure. Error bars indicate ± SD. ($n = 3$, three independent analyses of lipid extracts from three independent cultures).

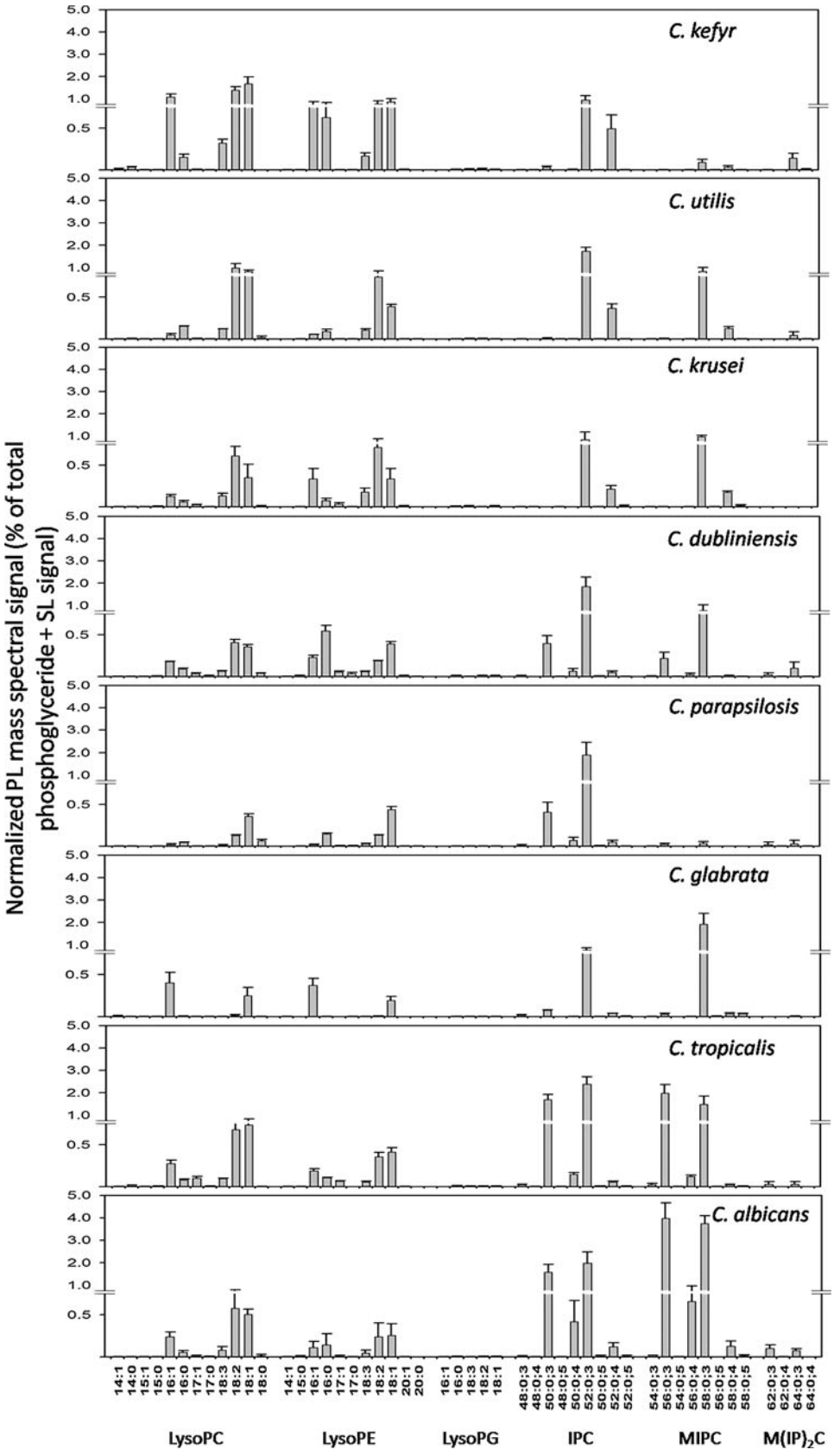

FIG. 5. Molecular lipid species compositions of major lyso-phosphoglycerides and SL groups (as percentage of the normalized total phosphoglyceride + SL mass spectral signals normalized to internal standards) in *Candida*. *Candida* species were cultured in YPD medium at 30°C as described in Materials and Methods. All the lyso-phospholipid and SL species analyzed are shown in this figure. Error bars indicate ± SD. ($n = 3$, three independent analyses of lipid extracts from three independent cultures.)

species identified as one of the 12 lowest loading components for principal component 1 is significantly higher in *C. glabrata* than in any of the other *Candida* species.

Principal component 2 differentiates several *Candida* species; for example, it describes the variation between *C. krusei* and *C. utilis* compared to *C. tropicalis*. The highest loadings for principal component 2 point to *C. tropicalis* having high levels of the most of the highest loading lipid species compared to *C. krusei* and *C. utilis*. Molecular species that are present at higher amounts in *C. tropicalis* than in *C. krusei* and *C. utilis* include PS 32:1, PEs 30:1, 31:1, and 31:2, and PCs 31:1 and 33:2. *C. krusei* and *C. utilis*, on the other hand, have high levels of lipids with the lowest loadings values, including PEs 37:0, 37:1, 36:4, and 36:5, LysoPEs 18:2 and 18:3, PC 36:5, PIs 36:4 and 36:5, and IPC 52:0;4 compared to *C. tropicalis*.

Principal component 3 describes the difference between *C. kefyr* and *C. parapsilosis* (Fig. 6B). The loading values for principal component 3 indicate that the separation between the two species reflect higher levels of several lysophosphoglycerides (LysoPC, LysoPE) in *C. kefyr* and higher levels of 36-carbon phosphoglycerides with one or two double bonds (PCs 36:1 and 36:2, PE 36:1 and 36:2, PAs 36:1 and 36:2, PG 36:1, and PS 36:1) in *C. parapsilosis*.

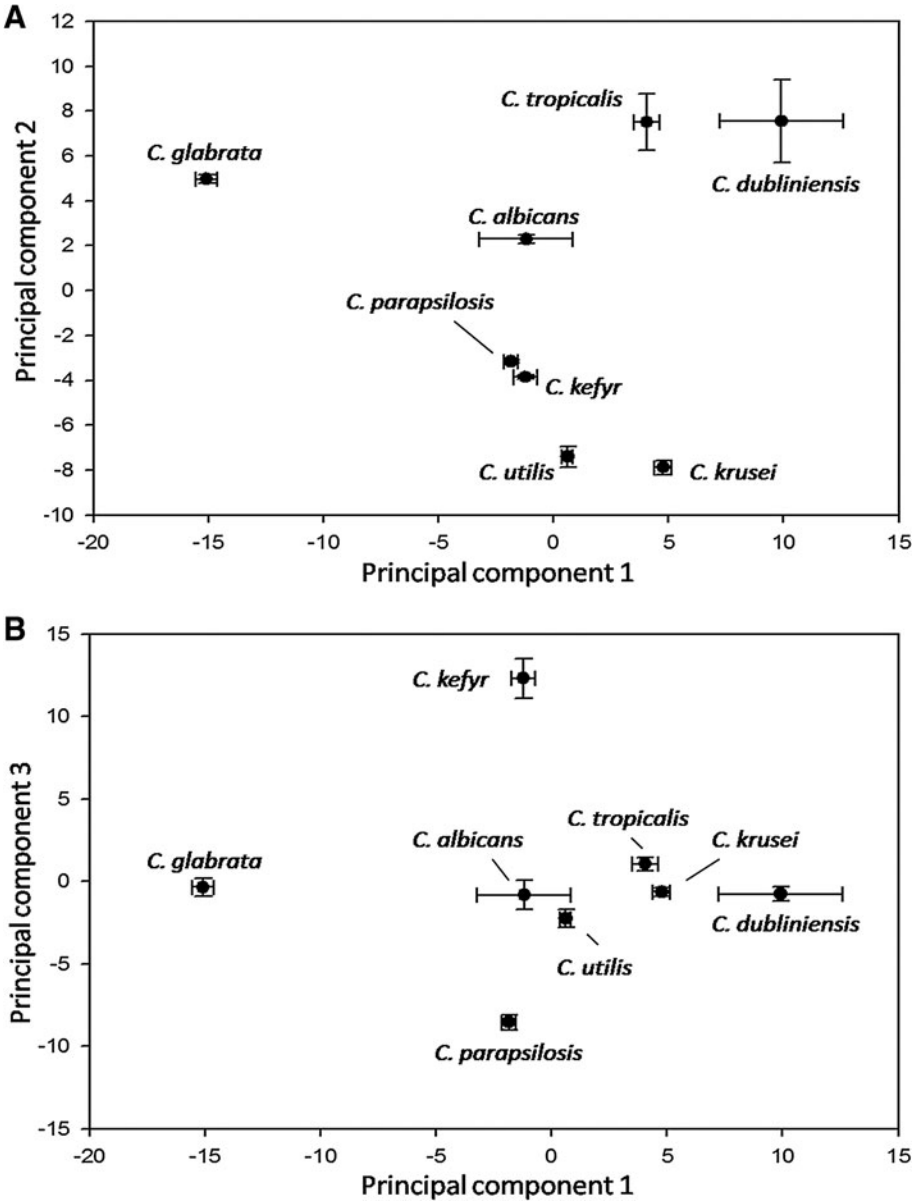

FIG. 6. Principal component analysis (PCA) of phospholipid species amongst eight *Candida* species. PCA was performed using the software SYSTAT, version 10 as described in Materials and Methods. The scores for the first three principal components, explaining 52.8% of the variance, were plotted. Each point in the plot is the mean of corresponding replicate's principal component scores. (**A**) The scores plot of principal component 1 (22.2% of variance) versus principal component 2 (16.9%). (**B**) The scores plot of principal component 1 (22.2%) vs principal component 3 (13.7% of variance).

Table 2. Loadings of Principal Components 1, 2, and 3

Lipid species 1	*Principal component 1 loadings*	*Lipid species 2*	*Principal component 2 loadings*	*Lipid species 3*	*Principal component 3 loadings*
Twelve lowest loading values					
PC 30:2	−0.840	PI 34:1	−0.722	PC 36:2	−0.787
PI 36:1	−0.833	LysoPE 18:2	−0.686	PE 36:2	−0.783
PC 32:2	−0.832	PE 37:0	−0.675	PA 36:2	−0.691
PE 32:2	−0.824	PI 36:4	−0.668	PE 36:1	−0.687
PE 30:2	−0.801	PE 36:5	−0.655	PC 36:1	−0.671
PC 34:2	−0.789	PE 36:4	−0.651	LysoPC 18:0	−0.661
PA 32:2	−0.786	LysoPE 18:3	−0.641	PE 38:2	−0.650
PI 32:2	−0.785	PE 37:1	−0.636	PE 36:3	−0.643
PC 32:0	−0.765	IPC 52:0;4	−0.635	PA 36:1	−0.642
PE 34:2	−0.746	PC 36:5	−0.622	PG 36:1	−0.622
PI 38:1	−0.708	PI 36:5	−0.610	PC 34:1	−0.606
PE 26:1	−0.686	PC 34:1	−0.569	PS 36:1	−0.560
Twelve highest loadings values					
LysoPE 17:1	0.703	PS 35:2	0.701	PI 34:3	0.765
PS 36:4	0.705	PE 32:1	0.703	PA 36:6	0.781
PI 33:1	0.713	PA 34:2	0.708	LysoPC 18:1	0.788
LysoPG 16:0	0.723	PE 30:1	0.710	PA 34:4	0.793
PE 38:6	0.726	PA 32:1	0.720	PI 35:0	0.808
PI 35:2	0.730	PC 31:1	0.729	LysoPC 14:0	0.822
PG 36:3	0.737	PI 31:1	0.730	PI 30:2	0.837
PC 36:4	0.760	PC 33:2	0.732	$M(IP)_2C$ 64:0;4	0.843
PC 36:3	0.784	IPC 48:0;3	0.745	LysoPC 18:3	0.846
PE 38:4	0.792	PE 31:2	0.766	LysoPE 16:1	0.863
PE 37:2	0.795	PE 31:1	0.768	PI 34:4	0.880
PG 36:5	0.852	PS 32:1	0.815	LysoPC 16:1	0.907

The 12 highest and 12 lowest values are indicated.

Discussion

Lipidomics is a targeted metabolomics platform which provides comprehensive analysis of lipid species with high sensitivity. In this study, we have performed a comparative lipidomics analysis of *Candida* species. This high throughput MS based analysis employed in this study is quicker ($\sim$60 min per sample) than conventional analytical methods (Carrasco-Pancorbo et al., 2009); it involved direct infusion of lipid extracts into the MS and required minimal sample preparation. We could identify and quantify phospholipid molecular species and perform interspecies comparison of the phospholipidome of *Candida* species. We determined the abundance of 223 molecular lipid species belonging to 12 major groups of PLs, which also include some lesser abundant lipid groups such as $M(IP)_2C$ and lysophosphoglycerides. Still, the analysis is not fully comprehensive as, for example, cardiolipin (CL) was not analyzed. By collision- induced dissociation, CL molecular ions fragment to produce several different fragments containing glycerol and phosphate. The lack of mass spectral fragments unique to CL and the multiple fragmentation pathways make analysis of this tetra-acyl glycerolipid by direct infusion tandem MS methods challenging.

PC, PE, and PI accounted for approximately 80% of the measured PLs, which included 108 molecular species. IPCs and MIPCs were the major *Candida* SLs measured. $M(IP)_2Cs$ produced only low amounts of mass spectral signal in all *Candida* species, suggesting that *Candida* may be lower in these SLs than nonpathogenic yeasts like *S. cerevisiae* (Ejsing et al., 2009).

Apart from identifying the major PL groups, this analysis also highlights the key features that define the lipidome of *Candida*. For example, although lipids containing odd-chain FA were not abundant, the analysis confirmed their presence, and thus provided support for the existence of an active odd-chain FA biosynthetic pathway in *Candida* species (Iida et al., 1980; Tahoun et al., 1988; White et al., 1988). The presence of polyunsaturated FA-containing lipids (18:2, 18:3, etc.) similarly confirmed the presence of active FA desaturases

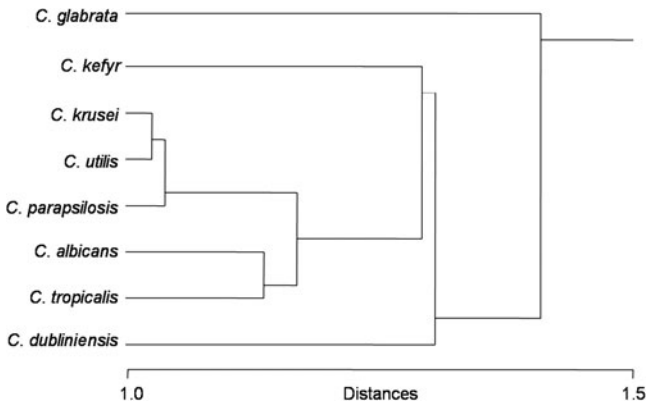

FIG. 7. Hierarchical cluster dendrogram for *Candida* species based on the phospholipidome profiles. Analysis was performed using the software SYSTAT, version 10 as described in Materials and Methods.

(Krishnamurthy et al., 2004). Taken together, these variations reflect the complexity of *Candida* lipidome.

Some *Candida* species possess unique PL molecular species profiles. For example, *C. glabrata* was more limited in its molecular species than other *Candida* species, with *C. glabrata* being particularly enriched in phosphoglycerides with only one or two double bonds in the two acyl chains. Lysophosphoglyceride and SLs species also varied in abundance among species. The distinguishing patterns suggest that each species of *Candida* has a distinctive lipid profile.

We have clustered PL profiles of a single strain from different *Candida* species (Fig. 7). The clustering reflects the very distinctive PLs of *C. glabrata* compared to other *Candida* species. *C. kefyr* and *C. dubliniensis* have different lipids but are part of the same cluster. *C. albicans* and *C. tropicalis*, on one hand, and *C. krusei*, *C. utilis* and *C. parapsilosis*, on the other hand, are similar in their lipid profiles and are thus clustered together. PCA proved to be a useful tool to highlight lipid variation among these species. However, a comparison with the hierarchical trees based on nuclear 18S rDNA, 26S rDNA, and complete genome sequences of fungal species (Diezmann et al., 2004; Fitzpatrick et al., 2006), revealed that *C. albicans* and *C. dubliniensis* are very closely related. However, lipidomic analyses suggest them to be different. Similarly, although *C. tropicalis* and *C. parapsilosis* fall in the same cluster based on rDNA sequences, they differ from each other with respect to their lipidomes. In another example, *C. glabrata* is closely related to *C. kefyr* based on rDNA sequences (Diezmann et al., 2004), but has drastically different lipidome profile compared to other *Candida* species. Thus it is apparent that clustering based on genome sequences and lipidomic profiles may not necessarily match in *Candida* species.

Conclusion

In *Candida*, lipid metabolism has been a prime target for strategies that kill these pathogenic organisms. However, increasing cases of MDR against the known antifungal drugs demand better drug targets, and emphasis has been placed again on lipid metabolic enzymes as potential targets. One roadblock has been identifying lipid biosynthetic pathways that might provide appropriate targets, partly because we have lacked the ability to analyze the functions of these pathways in a high-throughput manner. Our new ability to examine *Candida* lipids in greater depth, using MS-based approaches, should prove useful in analysis of drug targets.

Acknowledgments

The work presented in this article has been supported in part by grants to R.P. from Department of Biotechnology (BT/PR9100/Med/29/03/2007, BT/PR9563/BRB/10/567/2007, and BT/PR11158/BRB/10/640/2008). The lipid analyses described in this work were performed at the Kansas Lipidomics Research Center Analytical Laboratory, where equipment acquisition and method development were funded by the National Science Foundation (EPS 0236913, MCB 0455318, and DBI 0521587), Kansas Technology Enterprise Corporation, K-IDeA Networks of Biomedical Research Excellence (INBRE) of National Institute of Health (P20RR16475), the Johnson Cancer Center, and Kansas State University. A.S. is thankful to University Grants Commission, and Council of Scientific and Industrial Research, Government of India, for junior research fellowships award and American Society of Microbiology for providing ASM International fellowship for Asia to work at the Kansas Lipidomics Research Center Analytical Laboratory. A.S. acknowledges expert help from Richard Jeannotte. We acknowledge Advanced Instrumentation Research Facility (AIRF), JNU for providing GC-MS and technical assistance therein by Ajay Kumar.

Author Disclosure Statement

No competing financial interests exist between the authors of this article.

References

Bleijerveld, O.B., Houweling, M., Thomas, M.J., and Cui, Z. (2006). Metabolipidomics: profiling metabolism of glycerophospholipid species by stable isotopic precursors and tandem mass spectrometry. Anal. Biochem. 352, 1–14.

Bligh, E.G., and Dyer, W.J. (1959). A rapid method of total lipid extraction and purification. Can. J. Biochem. Physiol. 37, 911–917.

Carrasco-Pancorbo, A., Navas-Iglesias, N., and Cuadros-Rodríguez, L. (2009). From lipid analysis towards lipidomics, a new challenge for the analytical chemistry of the 21st century. Part I: modern lipid analysis. Trends Anal. Chem. 28, 263–278.

Dembitskii, V.M., and Pechenkina, E.E. (1991). Phospholipid and fatty-acid compositions of higher fungi. Chem. Nat. Compd. 27, 155–156.

Devaiah, S.P., Roth, M.R., Baughman, E., Li, M., Tamura, P., Jeannotte, R., et al. (2006). Quantitative profiling of polar glycerolipid species from organs of wild-type *Arabidopsis* and a phospholipase Dalpha1 knockout mutant. Phytochemistry 67, 1907–1924.

Diezmann, S., Cox, C.J., Schonian, G., Vilgalys, R.J., and Mitchell, T.G. (2004). Phylogeny and evolution of medical species of *Candida* and related taxa: a multigenic analysis. J. Clin. Microbiol. 42, 5624–5635.

Ejsing, C.S., Sampaio, J.L., Surendranath, V., Duchoslav, E., Ekroos, K., Klemm, R.W., et al. (2009). Global analysis of the yeast lipidome by quantitative shotgun mass spectrometry. Proc. Natl. Acad. Sci. USA 106, 2136–2141.

Ferreira, C.R., Saraiva, S.A., Catharino, R.R., Garcia, J.S., Gozzo, F.C., Sanvido, G.B., et al. (2010). Single embryo and oocyte lipid fingerprinting by mass spectrometry. J. Lipid Res. doi:10.1194/jlr.D001768.

Fitzpatrick, D.A., Logue, M.E., Stajich, J.E. and Butler, G. (2006). A fungal phylogeny based on 42 complete genomes derived from supertree and combined gene analysis. BMC Evol. Biol. 6, 99.

Fonzi, W.A., and Irwin, M.Y. (1993). Isogenic strain construction and gene mapping in *Candida albicans*. Genetics 134, 717–728.

Gaspar, M.L., Aregullin, M.A., Jesch, S.A., Nunez, L.R., Villa-Garcia, M., and Henry, S.A. (2007). The emergence of yeast lipidomics. Biochim. Biophys. Acta 1771, 241–254.

Guan, X.L., and Wenk, M.R. (2006). Mass spectrometry-based profiling of phospholipids and sphingolipids in extracts from *Saccharomyces cerevisiae*. Yeast 23, 465–477.

Han, X., and Gross, R.W. (1994). Electrospray ionization mass spectroscopic analysis of human erythrocyte plasma membrane phospholipids. Proc. Natl. Acad. Sci. USA 91, 10635–10639.

Iida, M., Kobayashi, H., and Iizuka, H. (1980). Cellular fatty acids derived from normal alkanes by *Candida rugosa*. Z. Allg. Mikrobiol. 20, 449–457.

Kohli, A., Smriti, Mukhopadhyay, K., Rattan, A., and Prasad, R. (2002). In vitro low-level resistance to azoles in *Candida albicans* is associated with changes in membrane lipid fluidity and asymmetry. Antimicrob. Agents Chemother. 46, 1046–1052.

Krishnamurthy, S., Plaine, A., Albert, J., Prasad, T., Prasad, R., and Ernst, J.F. (2004). Dosage-dependent functions of fatty acid desaturase Ole1p in growth and morphogenesis of *Candida albicans*. Microbiology 150, 1991–2003.

Mago, N., and Khuller, G.K. (1990a). Biosynthesis of major phospholipids in *Candida albicans*. Curr. Microbiol. 20, 369–372.

Mago, N. and Khuller, G.K. (1990b). Subcellular localization of enzymes of phospholipid metabolism in *Candida albicans*. J. Med. Vet. Mycol. 28, 355–362.

Mahmoudabadi, A.Z., Boote, V., and Drucker, D.B. (2001). Characterization of polar lipids of oral isolates of *Candida*, *Pichia* and *Saccharomyces* by Fast Atom Bombardment Mass Spectrometry (FAB MS). J. Appl. Microbiol. 90, 668–675.

Mukhopadhyay, K., Kohli, A., and Prasad, R. (2002). Drug susceptibilities of yeast cells are affected by membrane lipid composition. Antimicrob. Agents Chemother. 46, 3695–3705.

Mukhopadhyay, K., Prasad, T., Saini, P., Pucadyil, T.J., Chattopadhyay, A., and Prasad, R. (2004). Membrane Sphingolipid-Ergosterol interactions are important determinants of Multidrug Resistance in *Candida albicans*. Antimicrob. Agents Chemother. 48, 1778–1787.

Pasrija, R., Prasad, T., and Prasad, R. (2005). Membrane raft lipid constituents affect drug susceptibilities of *Candida albicans*. Biochem. Soc. Trans. 33, 1219–1223.

Pasrija, R., Panwar, S.L., and Prasad, R. (2008). Multidrug transporters CaCdr1p and CaMdr1p of *Candida albicans* display different lipid specificities: both ergosterol and sphingolipids are essential for targeting of CaCdr1p to membrane rafts. Antimicrob. Agents Chemother. 52, 694–704.

Prasad, R., and Kapoor, K. (2005). Multidrug resistance in yeast *Candida*. Int. Rev. Cytol. 242, 215–248.

Ringner, M. (2008). What is principal component analysis? Nat. Biotechnol. 26, 303–304.

Roberts, L.D., McCombie, G., Titman, C.M., and Griffin, J.L. (2008). A matter of fat: an introduction to lipidomic profiling methods. J. Chromatogr. B Anal. Technol. Biomed. Life Sci. 871, 174–181.

Tahoun, M.K., Shata, O.H., Mashalley, R.I., and Bou-Domia, S.A. (1988). Influence of selected sugars and temperature on fatty acids composition in *Candida tropicalis*. Nahrung 32, 327–333.

Van, M.G., Voelker, D.R., and Feigenson, G.W. (2008). Membrane lipids: where they are and how they behave. Nat. Rev. Mol. Cell Biol. 9, 112–124.

Watson, A.D. (2006). Lipidomics: A global approach to lipid analysis in biological systems. J. Lipid Res. 47, 2101–2111.

Welti, R., Li, W., Li, M., Sang, Y., Biesiada, H., Zhou, H.E., et al. (2002). Profiling membrane lipids in plant stress responses. Role of phospholipase D alpha in freezing-induced lipid changes in *Arabidopsis*. J. Biol. Chem. 277, 31994–32002.

Wenk, M.R. (2005). The emerging field of lipidomics. Nat. Rev. Drug Discov. 4, 594–610.

White, M.J., Hammond, R.C., and Rose, A.H. (1988). Effect of glucose and long-chain fatty acids on synthesis of long-chain alcohols by *Candida albicans*. J. Gen. Microbiol. 134, 2131–2137.

Address correspondence to:
Dr. Rajendra Prasad
School of Life Sciences
Jawaharlal Nehru University
Lab #101
New Delhi-110067, India

E-mail: rp47@mail.jnu.ac.in; rp47jnu@gmail.com